Expression and purification of human diacylglycerol kinase α from baculovirus-infected insect cells for structural studies

Daisuke Takahashi [1] , **Fumio Sakane** Corresp. [1]

[1] Department of Chemistry, Graduate School of Science, Chiba University, Chiba, Japan

Corresponding Author: Fumio Sakane
Email address: sakane@faculty.chiba-u.jp

Diacylglycerol kinases (DGKs) are lipid kinases that modulate the levels of lipid second messengers, diacylglycerol and phosphatidic acid. Recently, increasing attention has been paid to its α isozyme (DGKα) as a potential target for cancer immunotherapy. DGKα consists of the N-terminal regulatory domains including EF-hand motifs and C1 domains, and the C-terminal catalytic domain (DGKα-CD). To date, however, no structures of mammalian DGKs including their catalytic domains have yet been reported, impeding our understanding on the catalytic mechanism of DGKs and the rational structure-based drug design. Here we attempted to produce DGKα-CD or a full-length DGKα using bacterial and baculovirus-insect cell expression system for structural studies. While several DGKα-CD constructs produced using both bacterial and insect cells formed insoluble or soluble aggregates, the full-length DGKα expressed in insect cells remained soluble and was purified to near homogeneity as a monomer with yields (1.3 mg/mL per 1L cell culture) feasible for protein crystallization. Following enzymatic characterization showed that the purified DGKα is in fully functional state. We further demonstrated that the purified enzyme could be concentrated without any significant aggregation, and characterized its secondary structure by circular dichroism. Taken together, these results suggest that the presence of N-terminal regulatory domains suppress protein aggregation likely via their intramolecular interactions with DGKα-CD, and demonstrate that the baculovirus-insect cell expression of the full-length form of DGKα, not DGKα-CD alone, represents a promising approach to produce protein sample for structural studies of DGKα. Thus, our study will encourage future efforts to determine the crystal structure of DGK, which has not been determined since it was first identified in 1959.

1 **Expression and purification of human diacylglycerol kinase α from baculovirus-infected**

2 **insect cells for structural studies**

4 Daisuke Takahashi[1] and Fumio Sakane[1]*

6 [1]Department of Chemistry, Graduate School of Science, Chiba University, 1-33 Yayoi-cho,

7 Inage-ku, Chiba, 263-8522, Japan

9 *Corresponding author:

10   Fumio Sakane

11   Department of Chemistry, Graduate School of Science

12   Chiba University

13   1-33 Yayoi-cho, Inage-ku, Chiba, 263-8522, Japan

14   Tel.: +81-43-290-3695

15   Fax: +81-43-290-3695

16   Email: sakane@faculty.chiba-u.jp

17 **ABSTRACT**

18 Diacylglycerol kinases (DGKs) are lipid kinases that modulate the levels of lipid second

19 messengers, diacylglycerol and phosphatidic acid. Recently, increasing attention has been paid to

20 its α isozyme (DGKα) as a potential target for cancer immunotherapy. DGKα consists of the N-

21 terminal regulatory domains including EF-hand motifs and C1 domains, and the C-terminal

22 catalytic domain (DGKα-CD). To date, however, no structures of mammalian DGKs including

23 their catalytic domains have yet been reported, impeding our understanding on the catalytic

24 mechanism of DGKs and the rational structure-based drug design. Here we attempted to produce

25 DGKα-CD or a full-length DGKα using bacterial and baculovirus-insect cell expression system

26 for structural studies. While several DGKα-CD constructs produced using both bacterial and

27 insect cells formed insoluble or soluble aggregates, the full-length DGKα expressed in insect

28 cells remained soluble and was purified to near homogeneity as a monomer with yields (1.3

29 mg/mL per 1L cell culture) feasible for protein crystallization. Following enzymatic

30 characterization showed that the purified DGKα is in fully functional state. We further

31 demonstrated that the purified enzyme could be concentrated without any significant

32 aggregation, and characterized its secondary structure by circular dichroism. Taken together,

33 these results suggest that the presence of N-terminal regulatory domains suppress protein

34 aggregation likely via their intramolecular interactions with DGKα-CD, and demonstrate that the

35 baculovirus-insect cell expression of the full-length form of DGKα, not DGKα-CD alone,

36 represents a promising approach to produce protein sample for structural studies of DGKα. Thus,

37 our study will encourage future efforts to determine the crystal structure of DGK, which has not

38 been determined since it was first identified in 1959.

39

Introduction

40

41 Diacylglycerol (DG) and phosphatidic acid (PA) are important signaling lipids and regulate a

42 myriad of cellular events by modulating numerous signaling proteins (English, 1996; Stace &

43 Ktistakis, 2006; Griner & Kazanietz, 2007; Almena & Merida, 2011), including protein kinase C

44 (PKC) isoforms (Newton, 1997; Parekh, Ziegler & Parker, 2000; Griner & Kazanietz, 2007) and

45 Ras guanyl nucleotide-releasing protein (RasGRP) (Ebinu et al., 1998; Tognon et al., 1998) by

46 DG, and mammalian target of Rapamycin (mTOR) (Ávila-Flores et al., 2005) and

47 phosphatidylinositol (PI)-4-phosphate 5-kinase (PIP5K) (Moritz et al., 1992) by PA. DG kinases

48 (DGKs), which was first identified in 1959 (Hokin & Hokin, 1959), are a family of lipid kinase

49 that regulates the intracellular levels of DG and PA by phosphorylating DG into PA (Sakane et

50 al., 2007; Merida, Ávila-Flores & Merino, 2008; Shulga, Topham & Epand, 2011). Mammalian

51 DGK consists of ten isozymes (α, β, γ, δ, η, κ, ϵ, ζ, ι, and θ), classified in 5 subtypes featuring

52 distinct regulatory domains and a conserved catalytic domain (Sakane et al., 2007; Shulga,

53 Topham & Epand, 2011), and each DGK serves as a key downregulator and upregulator for the

54 DG and PA-mediated cellular signaling, respectively.

55   DGKα is the first-cloned DGK isozyme in mammals (Sakane et al., 1990) and has amino-

56 terminal regulatory domains including EF-hand motifs and C1 domains, and a carboxyl-terminal

57 catalytic domain (Fig. 1A). Recently, increasing attention has been paid to DGKα as a potential

58 target for anti-cancer treatments including cancer immunotherapy (Dominguez et al., 2013;

59 Purow, 2015; Sakane, Mizuno & Komenoi, 2016; Liu et al., 2016; Noessner, 2017). Expression

60 of DGKα has been reported to be upregulated in melanoma cells (but not in noncancerous

61 melanocytes) (Yanagisawa et al., 2007), lymphoma (Bacchiocchi et al., 2005), hepatocellular

62 carcinoma (Takeishi et al., 2012), breast cancer cells (Torres-Ayuso et al., 2014), and

63 glioblastoma cells (Dominguez et al., 2013) where DGKα promotes cancer cell survival,

64 proliferation, migration and invasion (Merida et al., 2017). siRNA knockdown of *DGKA* or

65 inhibition of DGKα by small molecule inhibitors for DGKs, R59022 and R59949, has

66 detrimental effects on the proliferation of glioblastoma cells, melanoma, breast cancer, and

67 cervical cancer cells (Yanagisawa et al., 2007; Dominguez et al., 2013). In T-lymphocytes, on

68 the other hand, DGKα is appreciated as a critical attenuator for immune response. DGKα is

69 highly expressed in T-cells and decreases membrane DG levels required for RasGRP1-dependent

70 activation of the Ras-Erk pathway (Jones, 2002). Furthermore, *in vitro* and *in vivo* studies have

71   uncovered that DGKα is responsible for T-cell hyporesponsive state known as anergy state

72   (Olenchock et al., 2006; Zha et al., 2006).

73   Using a high-throughput DGK assay, we have recently identified a novel DGKα-selective

74   inhibitor, CU-3, and revealed that this compound targets the catalytic domain of DGKα (Liu et

75   al., 2016). Indeed, this compound not only induced the apoptosis of HepG2 hepatocellular

76   carcinoma and HeLa cervical cancer cells as observed for other DGK inhibitors with lower-

77   selectivity (Dominguez et al., 2013), but also enhanced the production of interleukin-2 in Jurkat

78   T cells (Liu et al., 2016), illustrating a double-strike effect of DGKα inhibitors potentially

79   utilized for cancer immunotherapy (Noessner, 2017). However, despite these biological and

80   biomedical importance, no structure has been determined for the catalytic domains of any

81   mammalian DGKs, thus impeding the detailed understanding of DGK catalytic machinery and

82   substrate binding sites as well as the development and optimization of effective DGKα

83   inhibitors.

84   One of the greatest challenges for the structure determination of DGK isozymes lies in

85   producing enough and soluble proteins suitable for protein crystallization, as illustrated in

86   previous studies (Takahashi et al., 2012; Petro & Raben, 2013). Although intensive efforts have

87   been made by Petro *et al*. (Petro & Raben, 2013) to express and purify the full-length and

88   catalytic domain (CD) of porcine DGKα using bacterial expression system with expression-tags

89   (glutathione S-transferase (GST), maltose binding protein (MBP), thioredoxin (TRX)) for

90   solubility enhancement, all the expressed DGKα constructs formed inclusion bodies or soluble

91   aggregates, likely due to the inability of bacterial translational and folding machineries. To

92   overcome these problems, here we have taken advantage of the baculovirus-insect cell

93   expression system to express a full-length DGKα in soluble form. DGKα expressed in the insect

94   cells was then purified by a series of column chromatography, and the purified protein was found

95   to be a monomer in solution. Successful purification of DGKα also allowed us to characterize

96   enzymatic, inhibitory and structural properties of DGKα *in vitro*. Taken together, these results

97   provide promising evidence that the baculovirus-insect cell expression system is better suited to

98   produce DGKα for *in vitro* functional and structural studies.

99

100

101 **Materials & Methods**

102 **Bacterial expression and purification of DGKα-CD**

103 Multiple-constructs approach with different N- and C-terminal boundaries (Gräslund et al.,

104 2008), and several N-terminal fusion-tags (GST, MBP, and small ubiquitin-like modifier

105 (Sumo)) was applied for bacterial expression of DGKα-CD.

106   To prepare GST-fused constructs, the DNA sequences of DGKα-CD (S332–G722,

107 D344–G722, D369–G722, S332–S735, D344–S735, D369–S735,) flanked by *Bam*HI and *Sal*I

108 restriction sites were amplified by PCR from the full-length cDNA for human DGKα, inserted

109 into a pGEX-4T-2 vector (GE Healthcare) and the resulting plasmids were used to transform *E.*

110 *coli* strain Rosetta2 (DE3) (Novagen). The protein construct contained a thrombin-cleavable

111 GST-tag before the DGKα-CD sequence. Cells were cultured in LB media at 37°C until OD_{600}

112 reached 0.6–0.8. Expression of the recombinant protein was then induced by adding 0.5 mM

113 isopropyl β-D-thiogalactopyranoside (IPTG), and the bacterial culture was continued at 16°C for

114 overnight. Bacteria harvested by centrifugation were suspended in a lysis buffer (50 mM sodium

115 phosphate, pH 8.0, containing 500 mM NaCl, 1 mM phenylmethylsulfonyl fluoride, 1mM

116 dithiothreitol) and lysed by sonication on ice. Protease inhibitors (20 μg/mL aprotinin, 20 μg/mL

117 leupeptin, 20 μg/mL pepstatin, 1 mM soybean trypsin inhibitor) were added immediately before

118 sonication. To evaluate expression and solubility of the expressed proteins, soluble and insoluble

119 fractions were separated by centrifugation at 15,000 x g for 10 min and subjected to SDS-PAGE

120 (10%) followed by Coomassie Brilliant Blue (CBB) staining and immunoblot analysis using

121 anti-GST monoclonal antibody (B-14, Santa Cruz Biotechnology). The immunoreactive bands

122 were visualized using peroxidase-conjugated anti-mouse IgG antibodies (Jackson

123 ImmunoResearch Laboratories) and the ECL Western blotting detection system (GE Healthcare).

124   For Sumo-tag, the DNA sequences of DGKα-CD (S332–G722, D344–G722, D369–

125 G722, S332–S735, D344–S735, D369–S735) were cloned via *Nde*I/*Sal*I sites into pSUMO

126 vector. In addition, three constructs with additional two glutamic acids at the C-terminus (S332–

127 S735EE, D344–S735EE, D369–S735EE) were also cloned into the pSUMO vector. The

128 resulting recombinant protein contains an N-terminal His-tagged Sumo domain, followed by a

129 Sumo-specific protease (Ulp1) cleavage site before the DGKα-CD sequence. His_{x6}-Sumo-

130 DGKα-CD was expressed in *E. coli* Rosetta2 (DE3) cells by induction with 0.1 mM IPTG at

131 16°C for overnight. After a small-scale expression and solubility test using anti-His$_{x6}$

132 monoclonal antibody (9C11, Wako), large scale expression of the construct D344–S735EE was

133 conducted. After cell-lysis and centrifugation, Ni-affinity chromatography was applied to purify

134 His$_{x6}$-Sumo-DGKα-CD (D344–S735EE). The column was washed with 50 mM Tris-HCl, pH

135 8.0, 500 mM NaCl, 10 mM and 50 mM imidazole, and the bound proteins were eluted with 300

136 mM imidazole. An elution fraction containing His$_{x6}$-Sumo-DGKα-CD was concentrated using a

137 centrifugal filter (Amicon Ultra-15, Millipore), and applied to a Superdex 75 16/60 column for

138 size exclusion chromatography purification.

139   MBP-fused DGKα-CD constructs were prepared by cloning the sequences of DGKα-CD

140 (S332–G722, D344–G722, D369–G722, S332–S735, D344–S735, D369–S735, S332–S735EE,

141 D344–S735EE, D369–S735EE) into a pMAL-c2X vector (New England Biolabs) via

142 *Bam*HI/*Sal*I sites. *E. coli* strain Rosetta2 (DE3) transformed with the plasmids. Protein

143 expression was induced with 0.1 mM IPTG and bacterial cells were then incubated at 16°C for

144 overnight. After cell-lysis and centrifugation, the expression and solubility test was conducted by

145 subjecting soluble and insoluble fractions on SDS-PAGE (10%) followed by CBB staining and

146 immunoblot analysis using anti-MBP antibody (Sc-13564, Santa Cruz Biotechnology). The

147 construct MBP-DGKα-CD (D369–S735) was expressed in 2 L of LB medium and the MBP-

148 fused protein was purified by affinity chromatography on amylose resin (New England Biolabs).

149 The affinity column was washed with a buffer, 20 mM Tris-HCl, pH 7.4, 200 mM NaCl, 1 mM

150 phenylmethylsulfonyl fluoride, 1 mM EDTA, and the bound proteins were eluted with a buffer

151 containing 10 mM maltose. Fractions were subjected to SDS-PAGE (10%) and analyzed by CBB

152 staining and immunoblotting using anti-MBP antibody and anti-DGKα antibody (Yamada,

153 Sakane & Kanoh, 1989).

154 **Expression of DGKα in insect cells using baculovirus expression vector system**

155 The construct of DGKα-CD (D364–S735) or full-length DGKα with N-terminal His$_{x6}$ tag was

156 PCR-amplified and cloned into the pOET3 vector (Oxford Expression Technologies) via

157 *Sal*I/*Not*I sites. The resulting DNA sequences were verified to be correct by DNA sequencing.

158 The flashBAC system (Oxford Expression Technologies) was used to generate a recombinant

159 baculovirus and the virus stock was amplified by several rounds of infection of Sf9 cells cultured

160 in Sf-900 II serum free medium (Invitrogen) at a low multiplicity of infection (MOI). Plaque

161   assays were performed to determine titers of the amplified virus stocks. Both DGKα-CD and

162   full-length DGKα were expressed in Sf9 cells by infecting the cells (at 2×10^6 cells/ml) with the

163   baculovirus stock at MOI of 2. Cells were cultured at 28 °C with shaking for 24 hours and

164   pelleted by centrifugation at 1,500 x g, 4°C for 20 min and washed with sterile phosphate

165   buffered saline before storage at −80°C.

166   **Purification of DGKα expressed in insect cells**

167   The cell pellets were thawed and suspended in a lysis buffer containing 50 mM Tris-HCl, pH

168   8.0, 0.5 M NaCl, 20 mM imidazole, 20% glycerol, 5 mM $CaCl_2$, 5 mM $MgCl_2$, 5 mM β-

169   mercaptoethanol, 1% Nonidet P-40 (NP-40), 5 mM ADP, 5 U/mL benzonase (EMD Millipore)

170   and a EDTA-free protease inhibitor cocktail tablet (Roche). The cell suspension was lysed by

171   sonication on ice followed by centrifugation at 25,000 x g, 4°C for 1 hour. The supernatant was

172   incubated with 2 mL of Ni-NTA agarose (Qiagen) for 2 hours at 4°C, and then the mixture was

173   packed into a column by gravity. The column was washed with wash buffer 1 (50 mM Tris-HCl,

174   pH 8.0, 0.5 M NaCl, 20 mM imidazole, 20% glycerol, 5 mM $CaCl_2$, 5 mM $MgCl_2$, 5 mM β-

175   mercaptoethanol, 1% NP-40) and wash buffer 2 (50 mM Tris-HCl, pH 8.0, 0.5 M NaCl, 20 mM

176   imidazole, 20% glycerol, 5 mM $CaCl_2$, 5 mM $MgCl_2$, 5 mM β-mercaptoethanol and 10%

177   ethanol). Subsequently, the bound proteins were eluted with step-wise increase of imidazole

178   concentration (50, 100, and 200 mM) in a buffer consisting of 50 mM Tris-HCl, pH 8.0, 0.5 M

179   NaCl, 20 mM imidazole, 20% glycerol, 5 mM $CaCl_2$, 5 mM $MgCl_2$, 5 mM β-mercaptoethanol.

180   Collected fractions were analyzed by SDS-PAGE with Coomassie blue staining and immunoblot

181   analysis using anti-DGKα antibody (Yamada, Sakane & Kanoh, 1989).

182   Fractions containing full-length DGKα were further purified using size-exclusion

183   chromatography on a Superdex 200 column 16/60 equilibrated with 20 mM Tris-HCl, pH 7.4

184   with 200 mM NaCl, 3 mM $CaCl_2$, 3 mM $MgCl_2$, 0.5 mM dithiothreitol, and 5% glycerol.

185   Resulting fractions were analyzed by SDS-PAGE followed by Coomassie blue staining. Protein

186   quantification was done by Bradford assay or using the extinction coefficient, $E_{0.1\%} = 1.14$. Gel

187   filtration standards (Bio-Rad) containing thyroglobulin (670 kDa), γ-globulin (158 kDa),

188   ovalbumin (44 kDa), myoglobin (17 kDa), and vitamin B12 (1.3 kDa) were used to determine

189   the molecular mass of proteins.

190   *In vitro* **DGKα activity assay**

191   Activity of full-length DGKα was determined using the octyl-β-D-glucoside mixed micelle assay

192   combined with the ADP-Glo™ kinase assay kit (Promega), as previously described (Sato et al.,

193   2013; Liu et al., 2016). Briefly, the substrate micelle mixture containing 50 mM *n*-octyl-β-D-

194   glucoside (Dojindo), 10 mM (27 mol%) phosphatidylserine (PS; Sigma-Aldrich), 2 mM (5.4

195   mol%) 1,2-dioleolyl-*sn*-glycerol (DG; Sigma-Aldrich), 0.2 mM ATP in a final buffer consisting

196   of 50 mM MOPS, pH 7.4, 100 mM NaCl, 20 mM NaF, 10 mM $MgCl_2$, 1 µM $CaCl_2$ was mixed

197   with 5 µL of purified DGKα to initiate enzymatic reaction. The reaction mixtures were incubated

198   at 30°C for 30 min. Subsequently, 25 µL of ADP-Glo reagent was added and incubated at room

199   temperature for 40 min to terminate the enzyme reaction and deplete the remaining ATP. Kinase

200   Detection Reagent (50 µL) was then added to convert the ADP produced from the kinase

201   reaction into ATP for a luciferase/luciferin reaction. The reaction was performed at room

202   temperature for 40 min and the luminescence from the luciferase/luciferin reaction was measured

203   with a GloMax microplate reader (GloMax, Promega). A standard curve for ADP was generated

204   by fitting a various concentration of ADP ranging from 25 µM to 200 µM and the corresponding

205   luminescence signals (RLU) by linear regression, and was used to convert the luminescence

206   intensities from DGKα reaction into ADP concentrations. To determine kinetic constants, the

207   activity assay was performed under a series of concentrations of ATP (20 µM to 1 mM) and DG

208   (0 to 5.4 mol%), respectively. DGKα purified by size exclusion chromatography was added to

209   100 ng for each reaction and the assays were done in triplicate for each ATP or DG

210   concentrations. The K_m value was obtained by fitting the kinase activity of DGKα with the

211   Michaelis-Menten equation using Prism 7 (GraphPad). To test the calcium dependency of DGKα

212   activity, the enzyme activity was measured under the conditions containing either EGTA (3 mM)

213   or $CaCl_2$ (0.6 mM).

214   **Inhibitor activity assay**

215   Inhibitory activity of a previously identified inhibitor, CU-3 (Liu et al., 2016), against DGKα

216   was measured with the octyl-β-D-glucoside mixed micelle assay followed by the ADP-Glo

217   assay. A concentration series of CU-3 (0.02 to 10 µM) was incubated with the purified DGKα for

218   30 min at room temperature before adding to a reaction mixture for the assay. Half maximal

219 inhibitory concentration (IC50) was determined by fitting the CU-3 dependent decrease of

220 DGKα activity with the variable slope model in Graphpad Prism 7 software.

221 **Circular dichroism spectroscopy**

222 Circular dichroism (CD) spectrum were recorded at ambient conditions between 190 and 250 nm

223 on a Jasco J-805 spectrometer (Jasco Corporation) using a cell with path length of 0.2 mm, 20

224 nm/min scan speed and a bandwidth of 1 nm. DGKα was prepared at 0.32 mg/mL (3.75 μM) in

225 20 mM Tris-HCl buffer, pH 7.5, Ten spectra were averaged and a spectrum obtained for the

226 buffer was subtracted. Spectral data were analyzed using the program Contin-LL (Provencher &

227 Glöckner, 1981) suited in the DICHROWEB platform (Whitmore & Wallace, 2004).

228

229 **Results**

230 **A full-length form of DGKα was expressed in baculovirus-infected insect cells and purified**
231 **as a monomer**

232 We have previously reported that DGKα-CD possess enzymatic activity comparable to that of

233 the full-length enzyme when expressed in COS-7 cells (Sakane et al., 1996), indicating that its

234 substrate (ATP and DG) binding sites locate in the catalytic domain and DGKα-CD is an

235 essential target for inhibitor development. Full-length DGKα also contains cysteine-rich C1

236 domains (Fig. 1A), which might be detrimental for correct folding in heterologous expression

237 hosts. Therefore, we have first attempted to express DGKα-CD in *E.coli* by revamping the

238 previous approach by Petro *et al*. (Petro & Raben, 2013). In addition to N-terminal GST and

239 MBP-tags, which were previously utilized (Petro & Raben, 2013), we have used Sumo domain

240 fusion-tag for the enhancement of expression and solubility (Butt et al., 2005; Marblestone et

241 al.). To further increase the chance for expression of soluble proteins, we have also applied a

242 multiple-construct approach (Gräslund et al., 2008) to prepare DGKα-CD constructs which have

243 different N- and C-terminal boundaries (S332–G722, D344–G722, D369–G722, S332–S735,

244 D344–S735, D369–S735). Each of those constructs was fused with the GST, MBP, and Sumo-

245 tags. Despite our efforts, those constructs resulted in either insoluble inclusion body formation

246 (with GST-tag), or insufficient translation and proteolytic degradation (with MBP-tag), or

247 soluble microscopic aggregation (with Sumo-tag) (Fig. S1).

248   To circumvent the difficulty associated with bacterial expression system, we have used

249   baculovirus-infected Sf9 cells to produce DGKα-CD. The construct of DGKα-CD (D364–S735)

250   with N-terminal His$_{x6}$ tag was cloned into pOET3 transfer vector harboring the late AcMNPV

251   p6.9 promoter, which provides earlier expression compared to the polyhedrin promotor. The

252   recombinant DGKα-CD was expressed in cultured insect cells using the flashBAC baculovirus

253   vector expression system, and subsequently purified from cell-lysates using Ni-affinity

254   chromatography (Fig. S2A). Following size-exclusion chromatography on a Superdex 200,

255   however, demonstrated that DGKα-CD formed soluble aggregates eluting in the void volume of

256   the column (Fig. S2B).

257   In our early studies, a native form of full-length DGKα has been purified from porcine

258   thymus and this full-length form was found to be catalytically competent (Sakane, Yamada &

259   Kanoh, 1989; Sakane et al., 1991). We therefore set to produce full-length DGKα (aa 1–735)

260   using the same baculovirus expression system used for DGKα-CD. As expected, the vast

261   majority of DGKα remained in soluble form after cell lysis, as shown by immunoblot analysis

262   (Fig. 1B). Ni-affinity chromatography was conducted to purify DGKα from the cell lysis

263   supernatant, and relatively pure DGKα was eluted in fractions containing 50 mM and 100 mM

264   imidazole (Fig. 1C). To further purify DGKα, we next performed size-exclusion chromatography

265   on a Superdex 200 column. Because DGKα bears calcium-binding EF-hand motifs and a

266   magnesium ion was predicted to bind to the catalytic domain (Abe et al., 2003), we added 3 mM

267   CaCl$_2$ and 3 mM MgCl$_2$ in the equilibration buffer. DGKα eluted as a single peak at 73.5 mL

268   retention volume (Fig. 1D), which corresponds to the molecular mass of 77 kDa, based on a

269   calibration curve obtained with molecular mass standard proteins. This result indicates that

270   DGKα exists as a monomer in solution. DGKα was purified to near homogeneity (Fig. 1E) and

271   the yield was approximately 1.3 mg per 1L of Sf9 cell culture.

272   **Kinase activity assay and inhibitory assay for the purified DGKα**

273   To test whether the purified DGKα is catalytically active, we conducted the octyl-β-D-glucoside

274   mixed micelle assay combined with a luminescence-based assay that measures ADP produced in

275   a kinase reaction (Sato et al., 2013; Liu et al., 2016). DGKα purified from the size-exclusion

276   chromatography was found to exhibit kinase activity with peak fractions having the maximum

277   activity (Fig. 2A). We have previously demonstrated that DGKα activity, which has been

278   purified from porcine thymus or expressed in COS-7 cells, is enhanced by Ca^{2+} binding to its

279   two N-terminal EF-hand motifs (Sakane et al., 1990; 1991; Yamada et al., 1997). As predicted,

280   the purified DGKα exhibited significantly reduced activity when the bound calcium ions were

281   chelated with 5 mM EGTA (Fig. 2B). Furthermore, no significant changes of the activity were

282   observed after storage of the purified DGKα at 4°C for at least 3 months.

283   We also determined the kinetic parameters of DGKα for ATP and DG to assess the

284   catalytic properties of the purified DGKα. ATP-dependent increase of the kinase activity was

285   observed (Fig. 3A) and the K_m value was determined to be 0.24 ± 0.03 mM (Table 1),

286   comparable with those obtained with DGKα from porcine thymus (0.1 mM) (Sakane et al., 1991)

287   or DGKα expressed in COS-7 cells (0.1–0.25 mM) (Sato et al., 2013; Liu et al., 2016). The

288   activity was also increased in a DG-concentration dependent manner (Fig. 3B) and the K_m value

289   of 1.1 ± 0.21 mol% (Table 1) was consistent with those from our previous studies (3.3 mol%

290   with DGKα purified from porcine thymus (Sakane et al., 1991), 1.9–3.4 mol% with DGKα

291   expressed in COS-7 cells (Sato et al., 2013; Liu et al., 2016)). For both cases, compared to our

292   previous study using crude lysates of mammalian cells (Sato et al., 2013; Liu et al., 2016), the

293   relative activity increased nearly 50-fold when the purified DGKα was used. Furthermore, the

294   kinase activities of our purified DGKα (1–2 nmol/min/μg) is comparable to those obtained with

295   DGKα from porcine thymus (2.4 nmol/min/ μg) (Sakane et al., 1991). These results demonstrate

296   that the purified DGKα is in a fully functional state and stable during purification and storage.

297   We next measured the inhibitory activity of CU-3, a previously identified DGKα

298   inhibitor (Liu et al., 2016). CU-3 is an ATP competitive inhibitor with an IC_{50} value of 0.6 μM.

299   Consistent with this, CU-3 inhibited the activity of DGKα in a concentration-dependent manner

300   with an IC_{50} value of 0.34 ± 0.1 μM (Fig. 4).

301   **Structural characterization of the purified DGKα**

302   We also found that DGKα solution could be concentrated using a centrifugal filter without any

303   significant loss of the protein. Concentrated DGKα remained as a monomer as demonstrated by a

304   size-exclusion chromatography (Fig. S3). Using the concentrated DGKα (0.32 mg/mL), we

305   characterized the secondary structure using CD spectroscopy. The CD spectrum of DGKα and

306   following analysis indicates that DGKα is well-folded and contains certain amounts of α-helical

307   (18.9 %) and β-strand (27.4 %) structures (Fig. 5), further demonstrating that the expression of a

308   full-length DGKα, not a solo catalytic domain, in the baculovirus-infected insect cells is suitable

309   for producing a natively-folded and active form of DGKα.

310

Discussion

312   DGKs are a family of multi-domain lipid kinase that regulate a variety of cellular process

313   (Sakane et al., 2007; Merida, Ávila-Flores & Merino, 2008; Shulga, Topham & Epand, 2011),

314   and DGKα has recently emerged as a novel therapeutic target for cancer immunotherapy

315   (Dominguez et al., 2013; Purow, 2015; Sakane, Mizuno & Komenoi, 2016; Liu et al., 2016;

316   Noessner, 2017). However, no structural information of DGKs, especially their catalytic domain,

317   is available. This is largely because the procedure for large scale production of recombinant

318   DGKs in their soluble and homogeneous form, a prerequisite for protein crystallization, is not

319   well-established. Here we have used the baculovirus-insect cell expression system to produce a

320   full-length form (DGKα), and investigated the enzymatic and structural properties *in vitro*.

321   Petro and Raben have made significant efforts to express and purify a pig DGKα and

322   DGKα-CD using bacterial expression system with several fusion tags (GST, TRX, and MBP), a

323   set of bacterial chaperons, or *in-vitro* refolding (Petro & Raben, 2013). Despite their pursuit,

324   expressed DGKα constructs either formed inclusion bodies or soluble microscopic aggregates.

325   We have also used *E.coli* cells to produce DGKα-CD with several N-terminal fusion tags (GST,

326   Sumo, and MBP) and with different N- and C-terminal boundaries. While both MBP- and Sumo-

327   fused DGKα-CD remained in a soluble fraction after cell-lysis and Ni-affinity chromatography

328   (Fig. S1A and S1B), those DGKα-CD with fusion-tags eluted in the void volume of Superdex

329   200 column (Fig. S1C). When expressed with MBP, an elution fraction from the Ni-affinity

330   chromatography also contained additional smaller bands along with MBP-fused DGKα-CD (Fig.

331   S1A), which could be due to insufficient translational ability of *E.coli* for producing eukaryotic

332   proteins, as previously suggested (Petro & Raben, 2013). Because baculovirus-insect cell

333   expression system has both the capacity to produce recombinant proteins at a large scale and the

334   capability to provide eukaryotic protein expression machineries, we next utilized this system to

335   produce DGKα-CD. The protein expressed in Sf9 cells was soluble, however, contrary to our

336   expectation, the protein formed soluble aggregates, which eluted in the void volume (Fig. S2).

337   These results indicate that the only catalytic domain has a tendency to self-aggregate upon

338   isolation, possibly due to its intrinsic characteristics that recognize DG embedded in plasma

339   membrane, and suggest that the only catalytic domain is not suitable for structural studies even if

340   it is expressed using a eukaryotic expression system.

341   In contrast to the catalytic domain, full-length DGKα elutes in a relatively sharp peak of

342   size-exclusion chromatography and remains as a monomer when it is assumed to have a globular

343   shape (Fig. 1C and Fig. S3). Such production of a full-length DGKα in a soluble and monomeric

344   form using the baculovirus insect cell expression system holds promise for the preparation of

345   DGKα sample suitable for protein crystallization screening. DGKα consists of the N-terminal

346   regulatory domains including EF-hand motifs and C1 domains, and the C-terminal catalytic

347   domain. This suggests that DGKα adopts a compact globular structure rather than an elongated

348   one. YegS (a putative bacterial lipid kinase) (Bakali H, Nordlund & Hallberg, 2006), a bacterial

349   DgkB (Miller et al., 2008), and a human sphingosine kinase (SphK1) (Wang et al., 2013) have

350   been successfully purified and their crystal structures have been reported (Bakali H et al., 2007;

351   Miller et al., 2008; Wang et al., 2013). Although all of those lipid kinases are homologous to

352   mammalian DGKs and belong to a protein family PF00781 (*DAGK_cat*), they do not possess N-

353   terminal regulatory domains. This might explain why the N-terminal domain of DGKα is

354   required to obtain the protein as a soluble monomer. Interestingly, previous studies by us and

355   others have suggested the presence of intramolecular interactions between the N-terminal

356   regulatory domains and the catalytic domain (Merino et al., 2007; Takahashi et al., 2012). It is

357   reasonable to surmise that a potential aggregation-prone surface of the catalytic domain of

358   DGKα is intra-molecularly masked by the N-terminal regulatory domains including recoverin

359   homology, EF-hand motif, and C1 domains.

360   Enzymatic characterization of DGKα reveals that K_m values to ATP (0.24 mM) and DG

361   (1.1 mol%) are very similar to those obtained using DGKα partially purified from porcine

362   thymus (0.1 mM for ATP and 3.3 mol% for DG, respectively) (Sakane et al., 1991) or DGKα

363   expressed in COS-7 cells (0.1–0.25 mM for ATP and 1.9–3.4 mol% for DG, respectively) (Sato

364   et al., 2013; Liu et al., 2016), further demonstrating the effectiveness of baculovirus insect cell

365   expression system for producing DGKα not only in soluble and homogeneous form, but also in

366   its active one.

367

368   In summary, this study demonstrates that the production of full-length DGKα, not

369 DGKα-CD alone, using the baculovirus-insect cell expression is a very promising approach to

370 produce DGKα samples for future *in vitro* structural and functional studies. Firstly, DGKα has

371 been purified by Ni-affinity and size-exclusion chromatographies to near-homogeneity, and

372 purified DGKα remains in soluble and monomeric form, and can be concentrated without any

373 significant loss of the protein, which are prerequisites for protein crystallization. Purified DGKα

374 sample, however, still contains slight amounts of contaminant proteins which might non-

375 specifically bind to DGKα. Further modification and optimization of the protein construct and

376 purification conditions must be required. Secondly, the obtained yield of DGKα, 1.3 mg per 1L

377 cell culture, is enough to initiate crystal screening. Thirdly, the purified DGKα is catalytically

378 competent. The measured kinase activity and the K_m values to ATP and DG are comparable to

379 those obtained with native form of DGKα partially purified from porcine thymus and DGKα

380 expressed in mammalian cells.

381

Conclusion

383 We demonstrate that the baculovirus-insect cell expression of the full-length form of DGKα, not

384 DGKα-CD alone, represents a promising approach to produce protein sample suitable for

385 structural studies of DGKα. We believe that this study will encourage future pursuits to

386 determine crystal structures of mammalian DGKs that has still remained enigmatic for almost 60

387 years since its identification (Hokin & Hokin, 1959).

388

Acknowledgements

390 We thank Dr. Saurav Misra from Kansas State University for helpful suggestions regarding this

391 work. We thank Dr. Haobo Jiang from Oklahoma State University for providing pSUMO vector.

392 We thank Dr. Naoto Yonezawa (Chiba University) for giving Sf9 cells. We are grateful to Dr.

393 Takeshi Murata (Chiba University) for the use of their BioLogic chromatography system.

394

References

Abe T, Lu X, Jiang Y, Boccone CE, Qian S, Vattem KM, Wek RC, Walsh JP 2003. Site-directed mutagenesis of the active site of diacylglycerol kinase alpha: calcium and phosphatidylserine stimulate enzyme activity via distinct mechanisms. *Biochemical Journal* 375:673–680. DOI: 10.1042/BJ20031052.

Almena M, Merida I 2011. Shaping up the membrane: diacylglycerol coordinates spatial orientation of signaling. *Trends in Biochemical Sciences* 36:593–603. DOI: 10.1016/j.tibs.2011.06.005.

Ávila-Flores A, Santos T, Rincón E, Merida I 2005. Modulation of the mammalian target of rapamycin pathway by diacylglycerol kinase-produced phosphatidic acid. *Journal of Biological Chemistry* 280:10091–10099. DOI: 10.1074/jbc.M412296200.

Bacchiocchi R, Baldanzi G, Carbonari D, Capomagi C, Colombo E, van Blitterswijk WJ, Graziani A, Fazioli F 2005. Activation of alpha-diacylglycerol kinase is critical for the mitogenic properties of anaplastic lymphoma kinase. *Blood* 106:2175–2182. DOI: 10.1182/blood-2005-01-0316.

Bakali H MA, Herman MD, Johnson KA, Kelly AA, Wieslander A, Hallberg BM, Nordlund P 2007. Crystal structure of YegS, a homologue to the mammalian diacylglycerol kinases, reveals a novel regulatory metal binding site. *Journal of Biological Chemistry* 282:19644–19652. DOI: 10.1074/jbc.M604852200.

Bakali H MA, Nordlund P, Hallberg BM 2006. Expression, purification, crystallization and preliminary diffraction studies of the mammalian DAG kinase homologue YegS from Escherichia coli. *Acta Crystallographica Section F Structural Biology and Crystallization Communications* 62:295–297. DOI: 10.1107/S1744309106004799.

Butt TR, Edavettal SC, Hall JP, Mattern MR 2005. SUMO fusion technology for difficult-to-express proteins. *Protein Expression and Purification* 43:1–9. DOI: 10.1016/j.pep.2005.03.016.

Dominguez CL, Floyd DH, Xiao A, Mullins GR, Kefas BA, Xin W, Yacur MN, Abounader R, Lee JK, Wilson GM, Harris TE, Purow BW 2013. Diacylglycerol kinase α is a critical signaling node and novel therapeutic target in glioblastoma and other cancers. *Cancer Discovery* 3:782–797. DOI: 10.1158/2159-8290.CD-12-0215.

Ebinu JO, Bottorff DA, Chan EYW, Stang SL, Dunn RJ, Stone JC 1998. RasGRP, a Ras Guanyl Nucleotide- Releasing Protein with Calcium- and Diacylglycerol-Binding Motifs. *Science* 280:1082–1086. DOI: 10.1126/science.280.5366.1082.

English D 1996. Phosphatidic acid: A lipid messenger involved in intracellular and extracellular signalling. *Cellular Signalling* 8:341–347. DOI: 10.1016/0898-6568(95)00076-3.

Gräslund S, Nordlund P, Weigelt J, Bray J, Gileadi O, Knapp S, Oppermann U, Arrowsmith C, Hui R, Ming J, dhe-Paganon S, Park H-W, Savchenko A, Yee A, Edwards A, Vincentelli R, Cambillau C, Kim R, Kim S-H, Rao Z, Shi Y, Terwilliger TC, Kim C-Y, Hung L-W, Waldo GS, Peleg Y, Albeck S, Unger T, Dym O, Prilusky J, Sussman JL, Stevens RC, Lesley SA, Wilson IA, Joachimiak A, Collart F, Dementieva I, Donnelly MI, Eschenfeldt WH, Kim Y, Stols L, Wu R, Zhou M, Burley SK, Emtage JS, Sauder JM, Thompson D, Bain K, Luz J, Gheyi T, Zhang F, Atwell S, Almo SC, Bonanno JB, Fiser A, Swaminathan S, Studier FW, Chance MR, Sali A, Acton TB, Xiao R, Zhao L, Ma L-C, Hunt JF, Tong L, Cunningham K, Inouye M, Anderson S, Janjua H, Shastry R, Ho CK, Wang D, Wang H, Jiang M, Montelione GT, Stuart DI, Owens RJ, Daenke S, Schütz A, Heinemann U, Yokoyama S,

440   Büssow K, Gunsalus KC 2008. Protein production and purification. *Nature Methods* 5:135–
441   146. DOI: 10.1038/nmeth.f.202.
442   Griner EM, Kazanietz MG 2007. Protein kinase C and other diacylglycerol effectors in cancer.
443   *Nature reviews. Cancer* 7:281–294. DOI: 10.1038/nrc2110.
444   Hokin LE, Hokin MR 1959. Diglyceride phosphokinase: An enzyme which catalyzes the
445   synthesis of phosphatidic acid. *Biochimica et Biophysica Acta* 31:285–287. DOI:
446   10.1016/0006-3002(59)90481-0.
447   Jones DR 2002. Expression of a catalytically inactive form of diacylglycerol kinase a induces
448   sustained signaling through RasGRP. *The FASEB Journal*. DOI: 10.1096/fj.01-0762fje.
449   Liu K, Kunii N, Sakuma M, Yamaki A, Mizuno S, Sato M, Sakai H, Kado S, Kumagai K,
450   Kojima H, Okabe T, Nagano T, Shirai Y, Sakane F 2016. A novel diacylglycerol kinase α-
451   selective inhibitor, CU-3, induces cancer cell apoptosis and enhances immune response.
452   *Journal of Lipid Research* 57:368–379. DOI: 10.1194/jlr.M062794.
453   Marblestone JG, Edavettal SC, Lim Y, Protein PL 2006. Comparison of SUMO fusion
454   technology with traditional gene fusion systems: enhanced expression and solubility with
455   SUMO. *Protein Science* 15:182-189. DOI: 10.1110/ps.051812706.
456   Merida I, Ávila-Flores A, Merino E 2008. Diacylglycerol kinases: at the hub of cell signalling.
457   *Biochemical Journal* 409:1–18. DOI: 10.1042/BJ20071040.
458   Merida I, Torres-Ayuso P, Ávila-Flores A, Arranz-Nicolás J, Andrada E, Tello-Lafoz M,
459   Liébana R, Arcos R 2017. Diacylglycerol kinases in cancer. *Advances in Biological
460   Regulation* 63:22–31. DOI: 10.1016/j.jbior.2016.09.005.
461   Merino E, Sanjuán MA, Moraga I, Ciprés A, Merida I 2007. Role of the diacylglycerol kinase
462   alpha-conserved domains in membrane targeting in intact T cells. *Journal of Biological
463   Chemistry* 282:35396–35404. DOI: 10.1074/jbc.M702085200.
464   Miller DJ, Jerga A, Rock CO, White SW 2008. Analysis of the Staphylococcus aureus DgkB
465   Structure Reveals a Common Catalytic Mechanism for the Soluble Diacylglycerol Kinases.
466   *Structure* 16:1036–1046. DOI: 10.1016/j.str.2008.03.019.
467   Moritz A, De Graan PN, Gispen WH, Wirtz KW 1992. Phosphatidic acid is a specific activator
468   of phosphatidylinositol-4-phosphate kinase. *Journal of Biological Chemistry* 267:7207–
469   7210.
470   Newton AC 1997. Regulation of protein kinase C. *Current Opinion in Cell Biology* 9:161–167.
471   DOI: 10.1016/S0955-0674(97)80058-0.
472   Noessner E 2017. Diacylglycerol kinase-alpha: a checkpoint in cancer-mediated immuno-
473   inhibition and target for immunotherapy. *Frontiers in Cell and Developmental Biology*. DOI:
474   10.3389/fcell.2017.00016.
475   Olenchock BA, Guo R, Carpenter JH, Jordan M, Topham MK, Koretzky GA, Zhong X-P 2006.
476   Disruption of diacylglycerol metabolism impairs the induction of T cell anergy. *Nature
477   Immunology* 7:1174–1181. DOI: 10.1038/ni1400.
478   Parekh DB, Ziegler W, Parker PJ 2000. Multiple pathways control protein kinase C
479   phosphorylation. *The EMBO journal* 19:496–503. DOI: 10.1093/emboj/19.4.496.
480   Petro EJ, Raben DM 2013. Bacterial expression strategies for several Sus scrofa diacylglycerol
481   kinase alpha constructs: solubility challenges. *Scientific Reports* 3:352–14. DOI:
482   10.1038/srep01609.
483   Provencher SW, Glöckner J 1981. Estimation of globular protein secondary structure from
484   circular dichroism. *Biochemistry* 20:33–37. DOI: 10.1021/bi00504a006.
485   Purow B 2015. Molecular Pathways: Targeting Diacylglycerol Kinase Alpha in Cancer. *Clinical

486   *Cancer Research* 21:5008–5012. DOI: 10.1158/1078-0432.CCR-15-0413.

487 Sakane F, Imai S-I, Kai M, Yasuda S, Kanoh H 2007. Diacylglycerol kinases: why so many of
488   them? *Biochimica et Biophysica Acta* 1771:793–806. DOI: 10.1016/j.bbalip.2007.04.006.

489 Sakane F, Kai M, Wada I, Imai S-I, Kanoh H 1996. The C-terminal part of diacylglycerol kinase
490   alpha lacking zinc fingers serves as a catalytic domain. *Biochemical Journal* 318:583–590.

491 Sakane F, Mizuno S, Komenoi S 2016. Diacylglycerol Kinases as Emerging Potential Drug
492   Targets for a Variety of Diseases: An Update. *Frontiers in Cell and Developmental Biology*
493   4:82. DOI: 10.3389/fcell.2016.00082.

494 Sakane F, Yamada K, Kanoh H 1989. Different effects of sphingosine, R59022 and anionic
495   amphiphiles on two diacylglycerol kinase isozymes purified from porcine thymus cytosol.
496   *FEBS Letters* 255:409–413.

497 Sakane F, Yamada K, Imai S-I, Kanoh H 1991. Porcine 80-kDa diacylglycerol kinase is a
498   calcium-binding and calcium/phospholipid-dependent enzyme and undergoes calcium-
499   dependent translocation. *Journal of Biological Chemistry* 266:7096–7100.

500 Sakane F, Yamada K, Kanoh H, Yokoyama C, Tanabe T 1990. Porcine diacylglycerol kinase
501   sequence has zinc finger and E-F hand motifs. *Nature* 344:345–348. DOI:
502   10.1038/344345a0.

503 Sato M, Liu K, Sasaki S, Kunii N, Sakai H, Mizuno H, Saga H, Sakane F 2013. Evaluations of
504   the Selectivities of the Diacylglycerol Kinase Inhibitors R59022 and R59949 Among
505   Diacylglycerol Kinase Isozymes Using a New Non-Radioactive Assay Method.
506   *Pharmacology* 92:99–107. DOI: 10.1159/000351849.

507 Shulga YV, Topham MK, Epand RM 2011. Regulation and Functions of Diacylglycerol Kinases.
508   *Chemical Reviews* 111:6186–6208. DOI: 10.1021/cr1004106.

509 Stace CL, Ktistakis NT 2006. Phosphatidic acid- and phosphatidylserine-binding proteins.
510   *Biochimica et Biophysica Acta - Molecular and Cell Biology of Lipids* 1761:913–926. DOI:
511   10.1016/j.bbalip.2006.03.006.

512 Takahashi M, Yamamoto T, Sakai H, Sakane F 2012. Calcium negatively regulates an
513   intramolecular interaction between the N-terminal recoverin homology and EF-hand motif
514   domains and the C-terminal C1 and catalytic domains of diacylglycerol kinase Î±.
515   *Biochemical and Biophysical Research Communications* 423:571–576. DOI:
516   10.1016/j.bbrc.2012.06.006.

517 Takeishi K, Taketomi A, Shirabe K, Toshima T, Motomura T, Ikegami T, Yoshizumi T, Sakane
518   F, Maehara Y 2012. Diacylglycerol kinase alpha enhances hepatocellular carcinoma
519   progression by activation of Ras-Raf-MEK-ERK pathway. *Journal of Hepatology* 57:77–83.
520   DOI: 10.1016/j.jhep.2012.02.026.

521 Tognon CE, Kirk HE, Passmore LA, Whitehead IP, Der CJ, Kay RJ 1998. Regulation of
522   RasGRP via a Phorbol Ester-Responsive C1 Domain. *Molecular and Cellular Biology*
523   18:6995–7008. DOI: 10.1128/MCB.18.12.6995.

524 Torres-Ayuso P, Daza-Martín M, Martín-Pérez J, Ávila-Flores A, Merida I 2014. Diacylglycerol
525   kinase α promotes 3D cancer cell growth and limits drug sensitivity through functional
526   interaction with Src. *Oncotarget* 5:9710–9726. DOI: 10.18632/oncotarget.2344.

527 Wang Z, Min X, Xiao S-H, Johnstone S, Romanow W, Meininger D, Xu H, Liu J, Dai J, An S,
528   Thibault S, Walker N 2013. Molecular basis of sphingosine kinase 1 substrate recognition
529   and catalysis. *Structure* 21:798–809. DOI: 10.1016/j.str.2013.02.025.

530 Whitmore L, Wallace BA 2004. DICHROWEB, an online server for protein secondary structure
531   analyses from circular dichroism spectroscopic data. *Nucleic Acids Research* 32:W668–

532   W673. DOI: 10.1093/nar/gkh371.

533 Yamada K, Sakane F, Kanoh H 1989. Immunoquantitation of 80 kDa diacylglycerol kinase in
534   pig and human lymphocytes and several other cells. *FEBS Letters* 244:402–406.

535 Yamada K, Sakane F, Matsushima N, Kanoh H 1997. EF-hand motifs of α, β and γ isoforms of
536   diacylglycerol kinase bind calcium with different affinities and conformational changes.
537   *Biochemical Journal* 321:59–64.

538 Yanagisawa K, Yasuda S, Kai M, Imai S-I, Yamada K, Yamashita T, Jimbow K, Kanoh H,
539   Sakane F 2007. Diacylglycerol kinase α suppresses tumor necrosis factor-α-induced
540   apoptosis of human melanoma cells through NF-κB activation. *Biochimica et Biophysica*
541   *Acta - Molecular and Cell Biology of Lipids* 1771:462–474. DOI:
542   10.1016/j.bbalip.2006.12.008.

543 Zha Y, Marks R, Ho AW, Peterson AC, Janardhan S, Brown I, Praveen K, Stang S, Stone JC,
544   Gajewski TF 2006. T cell anergy is reversed by active Ras and is regulated by diacylglycerol
545   kinase-alpha. *Nature Immunology* 7:1166–1173. DOI: 10.1038/ni1394.

546

Enzyme kinetic parameters of DGKα with ATP and diaclyglycerol

1   **Table 1: Enzyme kinetic parameters of DGKα with ATP and diaclyglycerol**

Substrate	K_m	V_{max}
ATP	0.24 ± 0.03 mM	2.66 ± 0.15 nmol/min/µg
Diacylglycerol	1.06 ± 0.21 mol%	1.00 ± 0.06 nmol/min/µg

Figure 1

Expression of DGKα in baculovirus-infected insect cells and purification.

(A) Domain architecture of DGKα. RVH,recoverin homology domain; EF, EF-hand motif; C1, cysteine-rich C1 domain. **(B)** Immunoblot analysis of the solubility of a full-length DGKα expressed in Sf9 cells. Cell lysates were separated into supernatant and insoluble pellets and subjected to SDS-PAGE (10%) followed by immunoblot analysis using anti-DGKα antibody. **(C)** SDS-PAGE (10%) analysis of fractions from Ni^{2+}-affinity purification. Separated proteins were stained with Coomassie blue staining. **(D)** Elution profile of DGKα from size exclusion chromatography. Fractions numbers used for following SDS-PAGE analysis are labeled. The inset shows the calibration of gel-filtration column using protein standards of known molecular weight (thyroglobulin (670 kDa), γ-globulin (158 kDa), ovalbumin (44 kDa), myoglobin (17 kDa)). Partition coefficient (K_{av}) was calculated from the formula, $K_{av}=$ $(V_E–V_0)/(V_T–V_0)$, where V_E is the retention volume of each sample, V_T is the total column volume (120 mL), and V_0 is the void volume of the column (44 mL), respectively. K_{av} was plotted against the molecular weight of proteins and linear regression analysis was conducted. **(E)** SDS-PAGE (10%) analysis of DGKα purified using size-exclusion chromatography.

A

DGKα

RVH EF EF C1 C1 Catalytic domain

B

α-DGKα

100
85
67

(kDa)

Supernatant Pellets

C

Supernatant
Flow-through
Wash 1
Wash 2
Elution - 50 mM
Elution - 100 mM
Elution - 200 mM

137
117
100
85
67
50
34

(kDa)

← 85 kDa
His×6-DGKα

D

V_0 670 kDa 158 kDa 44 kDa 17 kDa

73.5 mL

0.015

0.010

A280

0.005

0.000

#6-7

Fractions #31-39

40 50 60 70 80 90 100 110

Retention volume (mL)

0.6 17 kDa
      44 kDa
0.4
Kav
      158 kDa
0.2
77 kDa   670 kDa

10^3 10^4 10^5

M.W. (Da)

E

Fraction numbers

Input 6 7 31 32 33 34 35 36 37 38 39

137
117
100
85
67
50
34

(kDa)

Figure 2

Purified DGKα is catalytically active and positively regulated by Ca^{2+}.

(A) Luminescence-based (ADP-glo) kinase activity assay of fractions from size exclusion chromatography of DGKα. Five microliters from each fraction containing 38.5 ng to 363 ng of DGKα was added for a reaction and the following details are described in Materials and Methods. Luminescence values are presented as relative luminescence unit (RLU) over background signals from a well containing a buffer (20 mM Tris-HCl, pH 7.4, 0.2 M NaCl, 3 mM $CaCl_2$, 3 mM $MgCl_2$, 0.5 mM DTT, and 5 % glycerol) used for size-exclusion chromatography. **(B)** Calcium-dependent activity of the purified DGKα. The luminescence-based DGK activity assay was conducted using 150 ng of DGKα in the presence of $CaCl_2$ (0.6 mM) and EGTA (3.6 mM). Purified DGKα was pre-incubated with 3 mM EGTA for 30 min on ice to chelate $CaCl_2$ contained in a buffer used for size exclusion chromatography, and concentrated EGTA was also added into the reaction mixture at a final concentration of 3.6 mM. Measured luminescence values of DGKα in the presence of $CaCl_2$ or EGTA were subtracted with each negative control ($CaCl_2$ or EGTA) and data shown are mean ± SD for triplicate measurements.

A
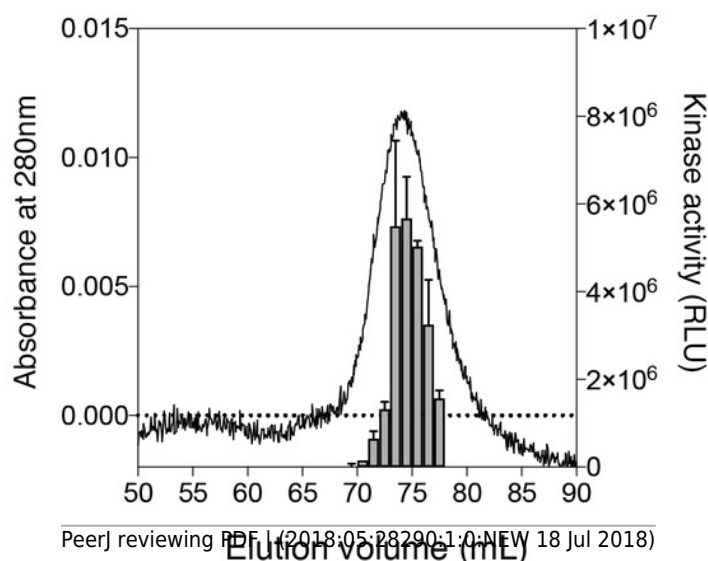
B
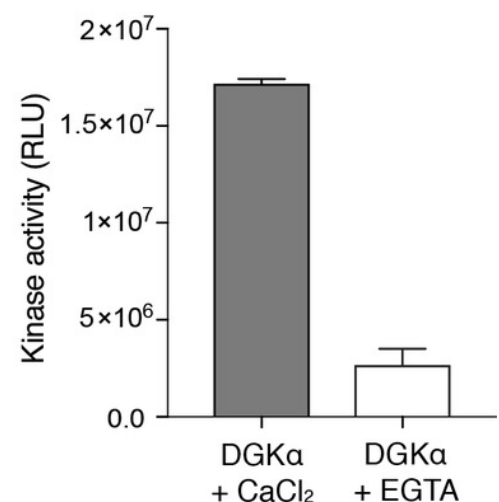
Figure 3

The enzymatic kinetics of the purified DGKα with ATP and diacylglycerol (DG).

(A) ATP dependency of DGKα activity was measured with the luminescence based assay. **(B)** DGKα activity was plotted as a function of DG concentration (mol%). Measured luminescence values were converted into the amount of ADP produced (nmol) based on the ATP-to-ADP conversion curve separately measured with known concentration of ATP (50 μM to 1 mM). Data shown are mean ± SD for triplicate measurements.
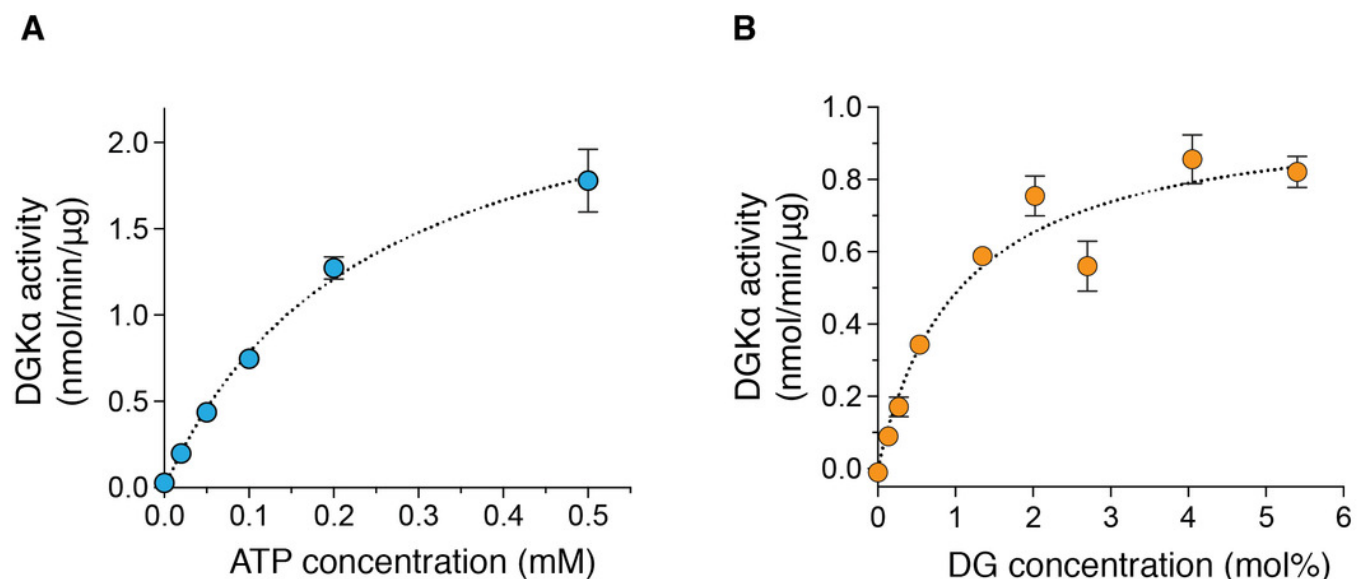
Figure 4

Inhibitory activity of a small molecule inhibitor, CU-3.

A concentration series of CU-3 ranging from 0.02 to 10 μM was incubated with the purified DGKα (100 ng) for 30 min at room temperature before adding to a reaction mixture for the mixed micelle/luminescence-based assay. Half maximal inhibitory concentration (IC_{50}) was determined by fitting the CU-3 dependent decrease of DGKα activity with the variable slope model. In the absence of DGKα, luminescence signals with various concentrations of CU-3 were negligible and no dose-dependent changes were observed.
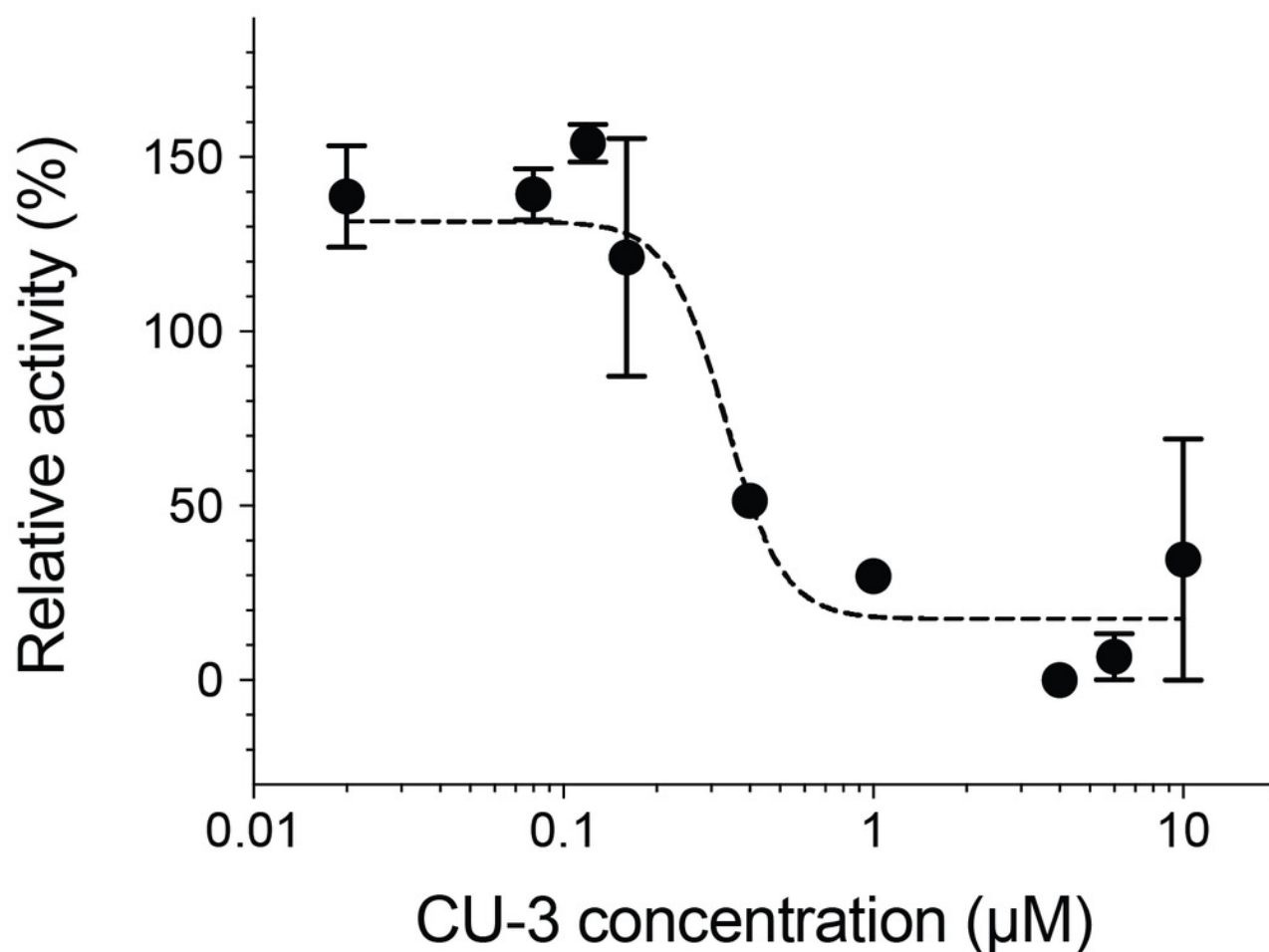
Figure 5

Secondary structure of the purified DGKα.

CD spectrum of DGKα measured at ambient conditions between 190 and 250 nm on a Jasco J-805 spectrometer. DGKα was prepared at 0.3 mg/mL in 20 mM Tris-HCl buffer, pH 7.4, 150 mM NaCl, 3 mM $MgCl_2$, 3 mM $CaCl_2$, 5 % glycerol. The analysis of the CD spectrum using the program Contin-LL (Provencher & Glöckner, 1981) suited in the DICHROWEB platform (Whitmore & Wallace, 2004) showed the presence of both α-helical (18.9 %) and b-strand (27.4 %) structures.